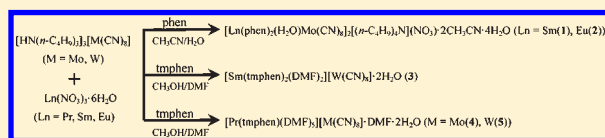


Syntheses, Structures, and Magnetic Properties of Five Novel Octacyanometallate-Based Lanthanide Complexes with Helical Chains

Su-Yan Qian,[†] Hu Zhou,[‡] Ai-Hua Yuan,^{*,†} and You Song^{*,§}[†]School of Biology and Chemical Engineering and [‡]School of Material Science and Engineering, Jiangsu University of Science and Technology, Zhenjiang 212003, People's Republic of China[§]State Key Laboratory of Coordination Chemistry, Nanjing National Laboratory of Microstructures, School of Chemistry and Chemical Engineering, Nanjing University, Nanjing 210093, People's Republic of China

S Supporting Information

ABSTRACT: The reactions of octacyanometallates $[M(CN)_8]^{3-}$ ($M = Mo, W$) and lanthanide ions Ln^{3+} ($Ln = Pr, Sm, Eu$) through the solution diffusion method in the presence of chelated aromatic ligands 1,10-phenanthroline (phen) or 3,4,7,8-tetramethyl-1,10-phenanthroline (tmphen) have yielded five new $[M(CN)_8]^{3-}$ -based bimetallic complexes with helical structures: $[Ln(phen)_2(H_2O)Mo(CN)_8]_2[(n-C_4H_9)_4N](NO_3) \cdot 2CH_3CN \cdot 4H_2O$ [$Ln = Sm(1), Eu(2)$], $[Sm(tmphen)_2(DMF)_2][W(CN)_8] \cdot 2H_2O$ (3), and $[Pr(tmphen)(DMF)_5][M(CN)_8] \cdot DMF \cdot 2H_2O$ [$M = Mo(4), W(5)$]. The Ln^{3+} centers are linked alternately by $[M(CN)_8]^{3-}$ units through two *trans* V-shaped cyano groups to form the left- and right-handed helical chains running along the screw axis. Magnetic measurements revealed the presence of an antiferromagnetic interaction between metal centers in 4 and 5.



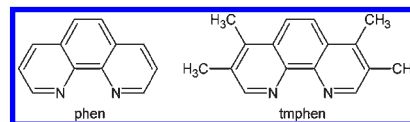
INTRODUCTION

Cyanometallates have received much attention in recent years, because of not only their fascinating variety of architectures and topologies¹ but also their tremendous potential applications as functional materials.² Of particular interest is the search for low-dimensional magnetic networks known as single molecule magnets (SMMs)³ or single chain magnets (SCMs),⁴ which exhibit slow relaxation of magnetization and are anticipated to exhibit quantum effects of magnetic properties. It should be mentioned here that there are only a rather limited numbers of examples⁵ when cyanide-based complexes with one-dimensional (1D) helical structures are focused on, implying a challenging issue in cyanide chemistry.

Indeed, the field of lanthanide helical complexes has been recently reviewed by C. Piguet et al.,⁶ and previous literature has demonstrated that a flexible or V-shaped bridging ligand is critical to the formation of helical frameworks.⁷ In addition, the chelated aromatic ligands are usually used to block coordination sites on metal ions, hence restricting the growth of the structure to finite dimensions rather than extended networks, and may provide potential supramolecular recognition sites for $\pi-\pi$ aromatic stacking interactions to form multistranded helices.^{7d,e}

Inspired by the aforementioned considerations and as a continuation of our research on the construction of cyano-bridged frameworks,^{1b,8} we chose versatile octacyanometallates $[M(CN)_8]^{3/4-}$ ($M = Mo, W$) as building blocks because the two adjacent V-shaped cyano groups are located at appropriate angles, which may allow $[M(CN)_8]^{3/4-}$ to connect metal ions to generate helical structural motifs. Thus, we assumed that magnetic $[M(CN)_8]^{3-}$ units could be useful in the formation of helical chains, reacting with lanthanide centers with flexible coordination

Scheme 1. Structures of the Ligands phen and tmphen



number, in the presence of chelated aromatic ligands 1,10-phenanthroline (phen) or 3,4,7,8-tetramethyl-1,10-phenanthroline (tmphen) (Scheme 1). Fortunately, foregoing efforts have led to the isolation of five novel octacyanometallate-based bimetallic complexes with helical structures (Scheme 2) $[Ln(phen)_2(H_2O)Mo(CN)_8]_2[(n-C_4H_9)_4N](NO_3) \cdot 2CH_3CN \cdot 4H_2O$ [$Ln = Sm(1), Eu(2)$], $[Sm(tmphen)_2(DMF)_2][W(CN)_8] \cdot 2H_2O$ (3), and $[Pr(tmphen)(DMF)_5][M(CN)_8] \cdot DMF \cdot 2H_2O$ [$M = Mo(4), W(5)$]. Magnetic properties of complexes 4 and 5 and the factors affecting the helical structure have been also discussed in this contribution. To our knowledge, 1–5 are the first examples of cyanide-bridged lanthanide complexes with helical structures.

EXPERIMENTAL SECTION

General Considerations. Unless otherwise mentioned, all reactants were used as purchased without further purification. IR spectra were measured on a Nicolet FT 1703X spectrophotometer in the 4000–400 cm^{-1} region using KBr pellets. All of the magnetization data were recorded on a Quantum Design MPMS-XL7 SQUID

Received: September 16, 2011

Revised: October 10, 2011

Published: October 11, 2011

Table 1. Crystallographic Data and Structural Refinements for 1–5

complexes	1	2	3	4	5
formula	C ₈₄ H ₈₆ Mo ₂ N ₂₈ O ₉ Sm ₂	C ₈₄ H ₈₆ Mo ₂ N ₂₈ O ₉ Eu ₂	C ₄₆ H ₅₀ N ₁₄ O ₄ SmW	C ₄₂ H ₆₂ MoN ₁₆ O ₈ Pr	C ₄₂ H ₆₂ WN ₁₆ O ₈ Pr
formula weight	2124.39	2127.61	1197.20	1155.93	1243.84
crystal system	tetragonal	tetragonal	monoclinic	monoclinic	monoclinic
space group	<i>I</i> ₄ / <i>acd</i>	<i>I</i> ₄ / <i>acd</i>	<i>P</i> ₂ ₁ / <i>c</i>	<i>P</i> ₂ ₁ / <i>c</i>	<i>P</i> ₂ ₁ / <i>c</i>
<i>a</i> (Å)	36.4209(18)	37.021(2)	15.2890(15)	16.9844(12)	17.0136(13)
<i>b</i> (Å)	36.4209(18)	37.021(2)	20.5000(16)	18.950(2)	19.237(3)
<i>c</i> (Å)	16.7366(16)	15.8242(18)	21.7150(12)	23.4842(16)	23.1634(15)
α (°)	90.00	90.00	90.00	90	90
β (°)	90.00	90.00	123.397(3)	125.795(3)	126.100(3)
γ (°)	90.00	90.00	90.00	90	90
<i>V</i> (Å ³)	22201(5)	21688(5)	5682.2(8)	6130.8(9)	6125.5(12)
<i>Z</i>	8	8	4	4	4
<i>D</i> _{calcd} (g cm ⁻³)	1.271	1.303	1.399	1.252	1.349
<i>M</i> (mm ⁻¹)	1.321	1.426	3.095	1.044	1.047
<i>F</i> (000)	8528	8544	2368	2364	2492
GOF on <i>F</i> ²	1.050	1.035	1.036	1.065	1.047
<i>R</i> ₁ / ω <i>R</i> ₂ [<i>I</i> > 2 σ (<i>I</i>)]	0.0340/0.0996	0.0400/0.1149	0.0532/0.1148	0.0503/0.1234	0.0423/0.0907
<i>R</i> ₁ / ω <i>R</i> ₂ (all data)	0.0461/0.1053	0.0532/0.1207	0.0783/0.1211	0.0636/0.1272	0.0546/0.0937

magnetometer. The molar magnetic susceptibilities were corrected for the diamagnetism estimated from Pascal's tables⁹ and for the sample holder by a previous calibration.

Syntheses of [Ln(phen)₂(H₂O)Mo(CN)₈]₂[(*n*-C₄H₉)₄N](NO₃)·2CH₃CN·4H₂O [Ln = Sm(1), Eu(2)]. Single crystals of **1** and **2** were prepared at room temperature in the dark by slow diffusion of a CH₃CN/H₂O (1:1) solution (3 mL) containing Ln(NO₃)₃·6H₂O (0.05 mmol) and phen (0.15 mmol) into a CH₃CN/H₂O (1:1) solution (15 mL) of [HN(*n*-C₄H₉)₃]₃[Mo(CN)₈]·4H₂O (0.05 mmol).¹⁰ After 3 weeks, yellow block crystals were obtained.

Synthesis of [Sm(tmphen)₂(DMF)₂][W(CN)₈]·2H₂O (3). Single crystals of **3** were prepared at room temperature in the dark by slow diffusion of a CH₃OH solution (3 mL) containing Sm(NO₃)₃·6H₂O (0.05 mmol) and tmphen (0.10 mmol) into a CH₃OH/DMF (3:1) solution (15 mL) of [HN(*n*-C₄H₉)₃]₃[W(CN)₈]·4H₂O (0.05 mmol).¹⁰ After 1 week, orange block crystals were obtained.

Syntheses of [Pr(tmphen)(DMF)₅][M(CN)₈]·DMF·2H₂O [M = Mo(4), W(5)]. Single crystals of **3** were prepared at room temperature in the dark by slow diffusion of a CH₃OH solution (3 mL) containing Pr(NO₃)₃·6H₂O (0.05 mmol) and tmphen (0.10 mmol) into a CH₃OH/DMF (3:1) solution (15 mL) of [HN(*n*-C₄H₉)₃]₃[M(CN)₈]·4H₂O (0.05 mmol). After 2 weeks, red block crystals were obtained. IR (KBr), $\nu_{\text{C}=\text{N}}$ for **4**: 2114, 2162 cm⁻¹; $\nu_{\text{C}=\text{N}}$ for **5**: 2139, 2163 cm⁻¹.

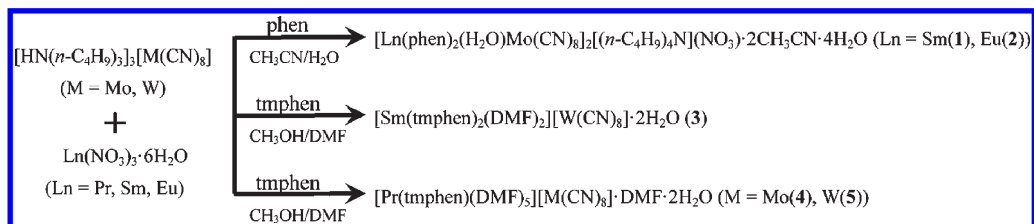
Crystallographic Data Collection and Structural Determination. Note here that the crystallized samples of **1–3** were very easy to pulverize to powders, with the occurrence of the phase transformation confirmed by powder X-ray diffraction analysis (Figure S1 in the Supporting Information). So, the samples of **1–3** used for other measurements (for example, IR, TG, and magnetism) are very difficult to obtain. We have used the following method when the single-crystal X-ray diffraction was performed: As soon as one well-shaped single crystal of **1–3** was removed from mother liquor, it was immediately introduced into a glass capillary having an open end and fixed. Then, the capillary was soon filled with the mother liquor and sealed for single-crystal X-ray structural determination. Diffraction data for **1–5** were collected on a Bruker Smart APEX II diffractometer equipped with Mo *K* α ($\lambda = 0.71073$ Å) radiation. Diffraction data analysis and reduction were performed within SMART, SAINT, and XPREP.¹¹ Correction for Lorentz, polarization, and absorption effects was performed within

SADABS.¹² Structures were solved using Patterson method within SHELXS-97¹³ and refined using SHELXL-97.¹⁴ All nonhydrogen atoms were refined with anisotropic thermal parameters. The H atoms of phen and tmphen ligands, acetonitrile, and DMF molecules, and the [(*n*-C₄H₉)₄N]⁺ cation were calculated at idealized positions and included in the refinement in a riding mode. For **1** and **2**, the H atoms bound to coordinated water molecule were located from difference maps and refined as riding, and the crystallized water molecule is disordered in three positions, each site being given occupancy factors of 0.3, 0.3 and 0.4, respectively. For **3**, the crystallized DMF molecule is disordered in two positions. The crystallographic data and experimental details for structural analyses of **1–5** are summarized in Table 1. Selected bond lengths and angles for **1–5** are listed in Table S1 in the Supporting Information.

RESULTS AND DISCUSSION

Crystal Structures. Single-crystal X-ray diffraction analysis revealed that complexes **1** and **2** are isostructural and crystallized in the tetragonal space group *I*₄/*acd*. Here, only the structure of **1** is described in detail. The asymmetric unit consists of one neutral [Sm(phen)₂(H₂O)Mo(CN)₈]₂ unit, one [(*n*-C₄H₉)₄N]⁺ cation, one NO₃⁻ anion, two crystallized CH₃CN molecules, and four solvent water molecules, as shown in Figure 1a. The eight-coordinated Mo center adopts a slightly square antiprism,¹⁵ where two *trans* V-shaped CN groups in [Mo(CN)₈]³⁻ are bridged to two adjacent Sm³⁺ centers, and the other six cyano groups are terminal. The average values of Mo–C and C–N bond distances are 2.144 and 1.201 Å, respectively, while the Mo–CN angles are nearly linear except for Mo1–C2N2 with 167.9(3)°. The coordination environment of Mo center is typical for the [Mo(CN)₈]³⁻-based complexes.¹⁶ The Sm center exhibits an eight-coordinated environment with two bridging cyano groups, two phen ligands, and two water molecules. The coordination geometry around Sm atom is a slightly distorted antiprism, in which the Sm–O and the mean Sm–N bond distances are 2.383 and 2.517 Å, respectively. The parameters of Sm center are comparable with related cyano-bridged dinuclear

Scheme 2. Syntheses of 1–5



complexes $\text{Sm}_2(\text{Ac})_2(\text{phen})_4(\text{H}_2\text{O})_2\{\text{Fe}(\text{CN})_5(\text{NO})\}_2$ ¹⁷ and $\{[\text{Sm}(\text{tmphen})_2(\text{H}_2\text{O})_2\text{M}(\text{CN})_6] \cdot \text{MeOH} \cdot n\text{H}_2\text{O}\}_\infty$ ($\text{M} = \text{Fe}, \text{Cr}$).¹⁸

Thus, the $[\text{Sm}(\text{phen})_2(\text{H}_2\text{O})]^{3+}$ cations in **1** are linked alternately by $[\text{Mo}(\text{CN})_8]^{3-}$ units through two *trans* V-shaped cyano groups [$\text{C1}-\text{Mo}-\text{C1}^1 = 144.0(2)^\circ$] to form the left- and right-handed helical chains running along the crystallographic 4_1 axis in the c direction with a pitch of 16.74 Å (Figure 1b). There are four $[\text{Sm}(\text{phen})_2(\text{H}_2\text{O})]^{3+}$ units and four $[\text{Mo}(\text{CN})_8]^{3-}$ moieties in each helical cycle. Interestingly, these chains are decorated with a pair of phen ligands alternately at two sides. It should be mentioned that the presence of two phen ligands with the dihedral angle of 74.29° coordinated to Sm atom has played a key role in the formation of 1D helical chains and also provided potential supramolecular recognition sites for $\pi-\pi$ aromatic stacking interaction. The intrachain $\text{Mo} \cdots \text{Sm}$ distance across the cyanide bridge is 5.756 Å. Viewed along the screw axis, the Sm and Mo atoms in a pitch form an eight-membered ring aperture (Figure 1c). The 1D helical chain exhibits an attractive structural framework with an unprecedented, very large diameter of approximately 12.945 Å, which is generated mainly by nitrate anions and solvent molecules serving as an efficient template. The guest species play an important role in the formation of single-stranded helical channels through specific host–guest interactions. The volume of solvent accessible voids is estimated to be 54% of the total volume in the crystal.¹⁹ In addition, the multipoint centroid-to-centroid and centroid-to-face separations of the neighboring phen segments from adjacent 1D helical chains are 3.747 and 3.644 Å, respectively, indicating the presence of strong $\pi-\pi$ stacking interactions between parallel phen planes.²⁰ As a consequence, adjacent achiral helices are racemically packed through $\pi-\pi$ intercalation of the phen aromatic rings into a 3D supramolecular network. Unlike other helical complexes reported previously,²¹ no hydrogen bonds or other weak interactions have been found in this system.

To study the overall factors affecting the structural framework of the cyanide systems, we varied the reaction conditions. When tmphen, a chelated aromatic ligand of a larger steric hindrance, was used instead of phen, analogous neutral single-stranded helices are formed in **3–5**.

Single-crystal X-ray diffraction measurements revealed that **3** crystallized in monoclinic system with space group $P2_1/c$. In the structure (Figure 2a), the $[\text{W}(\text{CN})_8]^{3-}$ unit takes an irregular square antiprism geometry, in which two cyanide groups bridge to the two neighboring Pr atoms, respectively, whereas the other six cyanide groups are terminal. The Pr center is eight-coordinated in a distorted square antiprismatic geometry made up by two bridged cyanide nitrogen atoms, four nitrogen atoms from two tmphen ligands, and two oxygen atoms form two coordinated DMF molecules. The dihedral angle 42.27° between the two benzene rings of tmphen is responsible for

the formation of the helical chain. Thus, the *trans* V-shaped cyanide groups [$\text{C1}-\text{W1}-\text{C6} = 144.5(3)^\circ$] bridge adjacent Sm and W centers to form the 1D right- and left-handed helical chains running along the crystallographic 2_1 axis in the b direction (Figure 2b). This chain is decorated by a pair of tmphen ligands above and below the helical chain. The pitch of 20.50 Å in **3** is significantly longer than that of 16.74 Å in **1** and **2**, which indicated that the different steric hindrance of chelated ligands can affect the spatial orientation of helical strands.

Because of the large steric requirement of the four substituted methyl groups, the single-stranded helix of **3** afforded a rhombic channel with a dimension of ca. $2.840 \text{ \AA} \times 2.596 \text{ \AA}$ (side distances) running parallel to the screw axis (Figure 2c), which is comparable to previously reported square or rectangular zinc helical channel.²² Two terminal cyano groups run through the channels. Neither isolated solvent molecules nor ions are found in these channels. It hints a possible method for designing a functional molecular channel, even though its effective void is quite small and of no practical use. Additionally, face-to-face (3.649 \AA) $\pi-\pi$ stacking interactions of tmphen extend the adjacent racemical helices into a 3D supramolecular network, and no hydrogen bonds or other weak interactions have been observed in **3**.

Single-crystal X-ray diffraction analysis revealed that **4** and **5** are isomorphous and crystallize in the monoclinic $P2_1/c$ space group. Here, only the structure of **4** is described in detail (Figure 3a). In the structure of **4**, each Mo atom has two bridging and six terminal cyano ligands arranged in a slightly distorted square antiprismatic geometry. The Pr center exhibits a nine-coordinated environment with two cyanonitrogens, two nitrogen atoms from one tmphen ligand, and four oxygen atoms from coordinated DMF molecules. The coordination geometry around Pr atom is a slightly distorted tricapped trigonal prism with the capping position occupied by N1, N4¹ [symmetry codes: (i) $-x + 2, y + 1/2, -z + 3/2$], and N10. Thus, Pr and Mo centers are linked in an alternating fashion to form a 1D neutral right- and left-handed helical chains running parallel to the crystallographic 2_1 screw axis (Figure 3b). It should be mentioned that the chain is decorated by only one tmphen ligand above and below the helical chain, which is different from a pair of chelated ligands in **1–3**. The single-stranded helix of **4** afforded a parallelogram channel (Figure 3c) with a dimension of ca. $3.519 \text{ \AA} \times 0.934 \text{ \AA}$ (side distances) running parallel to the screw axis with a pitch of 18.95 Å, as compared to the rhombic one in **3**.

The experimental results suggest that **3** and **5** exhibit some differences in the structure, although the same conditions was carried out expect for replacing Sm^{3+} with Pr^{3+} , which indicates that the structural changes of both complexes were induced by lanthanide metal ions.

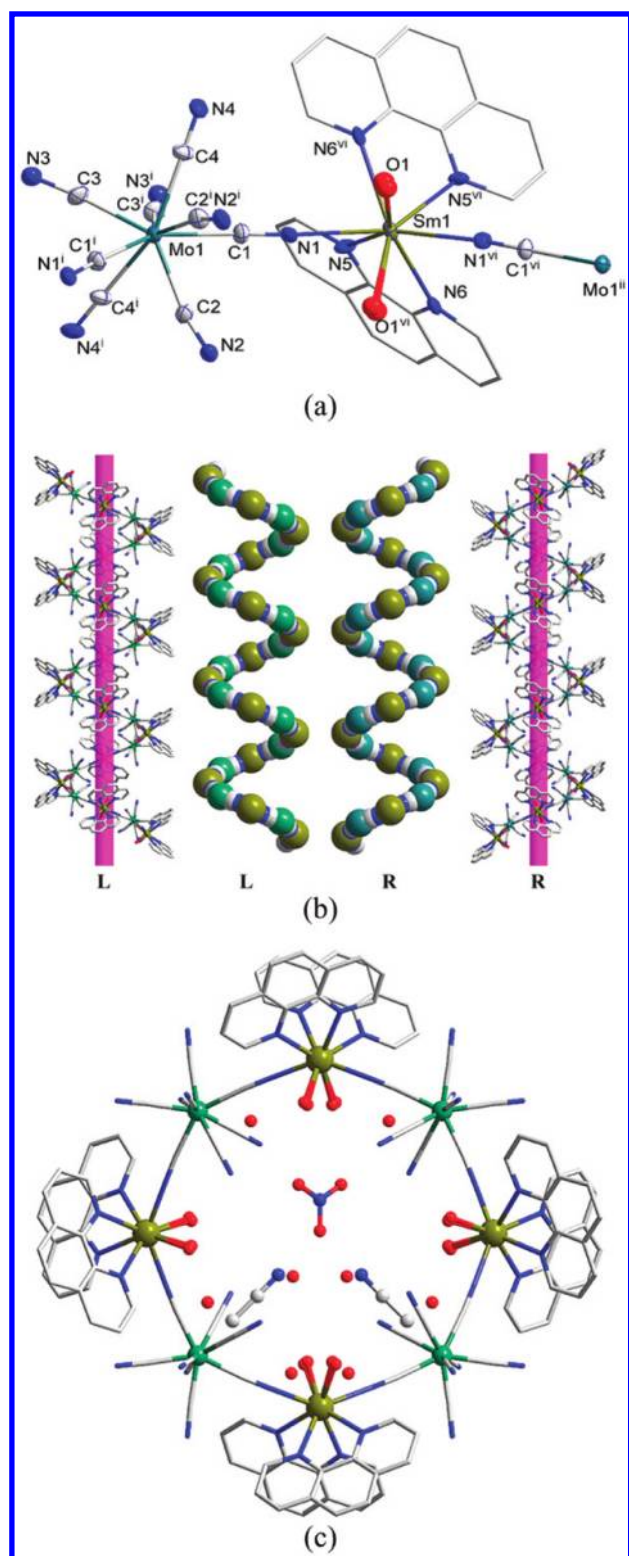


Figure 1. (a) ORTEP diagram of 1, showing the 30% probability thermal motion ellipsoid. All hydrogen atoms, $[(n-C_4H_9)_4N]^+$ cation, $[NO_3]^-$ anion, solvent CH_3CN , and H_2O molecules have been omitted for clarity. Symmetry codes: (i) $y - 1/4, x + 1/4, -z + 1/4$; (ii) $-y + 3/4, x - 1/4, -z + 1/4$; and (vi) $-x + 1/2, y, -z$. (b) Perspective and space-filling views of the racemic 1D helical structure of 1. (c) Perspective view of the single-stranded helix along the 4_1 screw axis of 1.

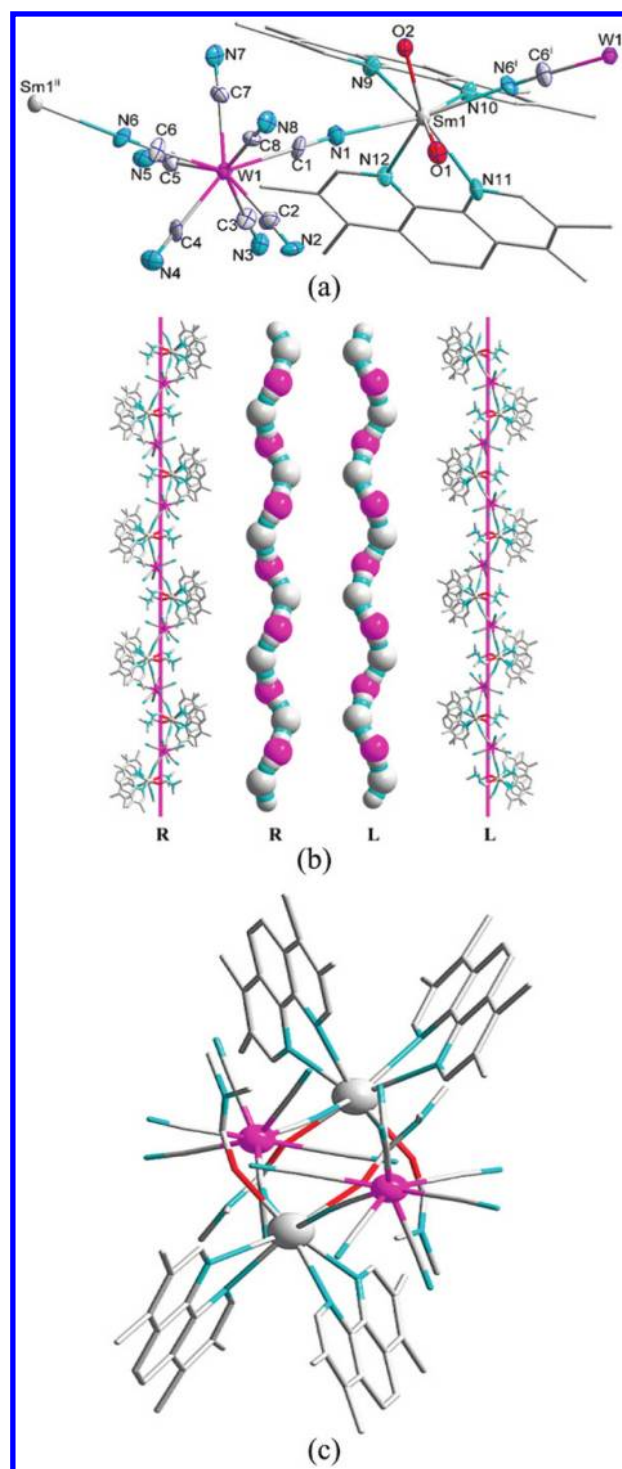


Figure 2. (a) ORTEP diagram of 3, showing the 30% probability thermal motion ellipsoid. All hydrogen atoms, crystallized water molecules, and carbon and nitrogen atoms of DMF have been omitted for clarity. Symmetry codes: (i) $-x + 2, y - 1/2, -z + 3/2$; and (ii) $-x + 2, y + 1/2, -z + 3/2$. (b) Perspective and space-filling views of the racemic 1D helical structure of 3. (c) Perspective view of the single-stranded helix along the 2_1 screw axis of 3.

Magnetic Properties. The temperature-dependent molar magnetic susceptibilities of 4 and 5 were measured in an applied field of 100 Oe, and their magnetic properties are very similar (Figure 4).

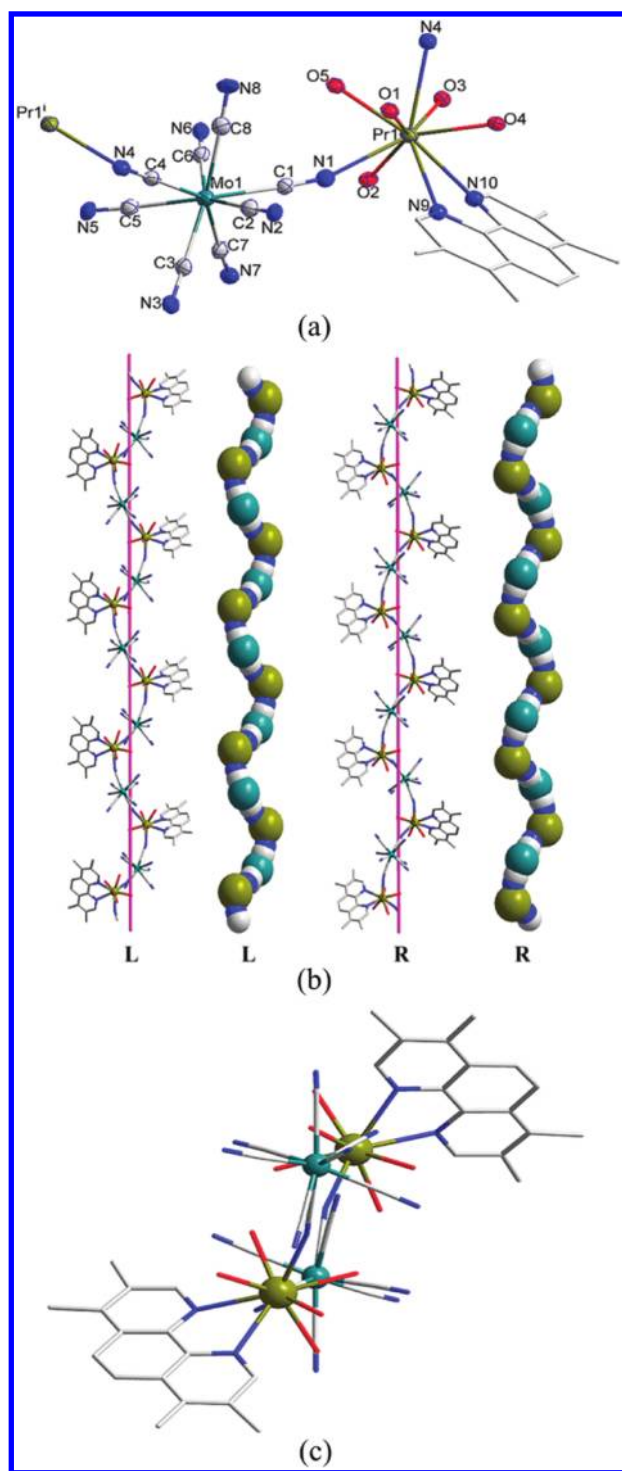


Figure 3. (a) ORTEP diagram of **4**, showing the 30% probability thermal motion ellipsoid. All hydrogen atoms, crystallized water molecules, and carbon and nitrogen atoms of DMF have been omitted for clarity. Symmetry codes: (i) $-x + 2, y + 1/2, -z + 3/2$. (b) Perspective and space-filling views of the racemic 1D helical structure of **4**. (c) Perspective view of the single-stranded helix along the 2_1 screw axis of **4**.

The values of χ_{MT} at 300 K are 1.936 and 1.847 $\text{cm}^3 \text{mol}^{-1} \text{K}$ for **4** and **5**, respectively. The χ_{MT} value for **5** is lower slightly than 1.98 $\text{cm}^3 \text{mol}^{-1} \text{K}$ expected for the isolated Pr^{III} ($J = 4, g_J = 4/5$) and W^{V} ($S = 1/2, g_S = 2$). Then, the curves display a smooth

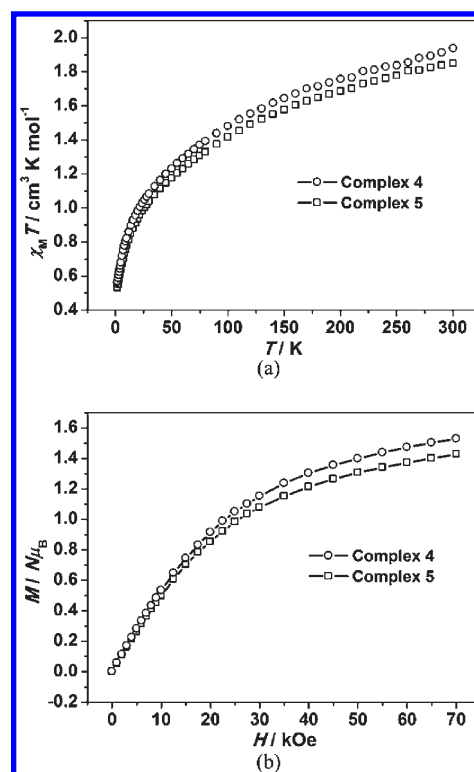


Figure 4. (a) Temperature dependence of χ_{MT} for **4** and **5** measured at 100 Oe. (b) Field dependence of the magnetization performed at 1.8 K for **4** and **5**.

monotonic decrease with a decrease in the temperature down to 1.8 K, due to the significant orbital contribution of Pr^{III} ion. The field dependence of the magnetization was measured at 1.8 K. The corresponding curves display a monotonic increase with an increasing value of the magnetic field and reach, at $H = 70$ kOe, the values of 1.53 and 1.42 $N\mu_B$ for **4** and **5**, respectively. These are significantly lower than the value of 3.85 $N\mu_B$ expected for the isolated Pr^{III} and M^{V} ions. All of these behaviors of complexes **4** and **5** are same as to that in the reference complex $[\text{Pr}^{\text{III}}(\text{terpy})(\text{DMF})_4][\text{W}^{\text{V}}(\text{CN})_8] \cdot 6\text{H}_2\text{O}$ reported by Sieklucka group,²³ so the coupling between Pr^{III} and Mo^{V} (or W^{V}) ions can simply be determined also to be antiferromagnetic.

CONCLUSION

In summary, we have presented the first cyanide-bridged lanthanide complexes (**1–5**) with helical chains by adopting an efficient and convenient protocol. The design idea depicted in this paper will be a promising technique for the construction of octacyanomethylate-based networks with helical characters, thus opening a new avenue in the exploration of SCMs. Efforts to explore the breadth and scope of this field are underway.

ASSOCIATED CONTENT

S Supporting Information. X-ray crystallographic data in CIF format of **1–5**, additional tables, and figures. This material is available free of charge via the Internet at <http://pubs.acs.org>.

Accession Codes

CCDC reference numbers: 785667 (**1**), 842868 (**2**), 785668 (**3**), 806360 (**4**), and 806361 (**5**).

AUTHOR INFORMATION

Corresponding Author

*E-mail: aihuayuan@163.com (A.-H.Y.) or yousong@nju.edu.cn (Y.S.).

ACKNOWLEDGMENT

This work was supported by National Natural Science Foundation of China (51072072, 51102119, and 91022031), Natural Science Foundation of Jiangsu Province (BK2010343 and BK2011518), and the Fundamental Research Funds for the Central Universities (1093020504).

REFERENCES

- (1) (a) Wang, X. Y.; Prosvirin, A. V.; Dunbar, K. R. *Angew. Chem., Int. Ed.* **2010**, *49*, 5081–5084. (b) Yuan, A. H.; Lu, R. Q.; Zhou, H.; Chen, Y. Y.; Li, Y. Z. *CrystEngComm* **2010**, *12*, 1382–1384. (c) Wang, J.; Zhang, Z. C.; Wang, H. S.; Kang, L. C.; Zhou, H. B.; Song, Y.; You, X. Z. *Inorg. Chem.* **2010**, *49*, 3101–3103. (d) Wang, Z. X.; Shen, X. F.; Wang, J.; Zhang, P.; Li, Y. Z.; Nfor, E. N.; Song, Y.; Ohkoshi, S.; Hashimoto, K.; You, X. Z. *Angew. Chem., Int. Ed.* **2006**, *45*, 3287–3291.
- (2) (a) Ohkoshi, S.; Imoto, K.; Tsunobuchi, Y.; Takano, S.; Tokoro, H. *Nat. Chem.* **2011**, *3*, 564–569. (b) Larionova, J.; Guari, Y.; Blanc, C.; Dieudonné, P.; Tokarev, A.; Guérin, C. *Langmuir* **2009**, *25*, 1138–1147. (c) Goodwin, A. L.; Calleja, M.; Conterio, M. J.; Dove, M. T.; Evans, J. S. O.; Keen, D. A.; Peters, L.; Tucker, M. G. *Science* **2008**, *319*, 794–797. (d) Arai, M.; Kosaka, W.; Matsuda, T.; Ohkoshi, S. *Angew. Chem., Int. Ed.* **2008**, *47*, 6885–6887. (e) Kaye, S. S.; Long, J. R. *J. Am. Chem. Soc.* **2005**, *127*, 6506–6507. (f) Sato, O.; Iyoda, T.; Fujishima, A.; Hashimoto, K. *Science* **1996**, *272*, 704–705. (g) Ferlay, S.; Mallah, T.; Ouahes, R.; Viellet, P.; Verdager, M. *Nature* **1995**, *378*, 701–703.
- (3) (a) Atanasov, M.; Comba, P.; Hausberg, S.; Martin, B. *Coord. Chem. Rev.* **2009**, *253*, 2306–2314. (b) Freedman, D. E.; Jenkins, D. M.; Iavarone, A. T.; Long, J. R. *J. Am. Chem. Soc.* **2008**, *130*, 2884–2885. (c) Yoon, J. H.; Lim, J. H.; Kim, H. C.; Hong, C. S. *Inorg. Chem.* **2006**, *45*, 9613–9615. (d) Lim, J. H.; Yoon, J. H.; Kim, H. C.; Hong, C. S. *Angew. Chem., Int. Ed.* **2006**, *45*, 7424–7426. (e) Berlinguette, C. P.; Vaughn, D.; Cañada-Vilalta, C.; Galán-Mascarós, J. R.; Dunbar, K. R. *Angew. Chem., Int. Ed.* **2003**, *42*, 1523–1526.
- (4) (a) Zhang, D. P.; Wang, H. L.; Chen, Y. T.; Ni, Z. H.; Tian, L. J.; Jiang, J. Z. *Inorg. Chem.* **2009**, *48*, 5488–5496. (b) Toma, L. M.; Lescouëzec, R.; Pasán, J.; Ruiz-Pérez, C.; Vaissermann, J.; Cano, J.; Carrasco, R.; Wernsdorfer, W.; Lloret, F.; Julve, M. *J. Am. Chem. Soc.* **2006**, *128*, 4842–4853. (c) Lescouëzec, R.; Toma, L. M.; Vaissermann, J.; Verdager, M.; Delgado, F. S.; Ruiz-Pérez, C.; Lloret, F.; Julve, M. *Coord. Chem. Rev.* **2005**, *249*, 2691–2729. (d) Lescouëzec, R.; Vaissermann, J.; Ruiz-Pérez, C.; Lloret, F.; Carrasco, R.; Julve, M.; Verdager, M.; Dromzee, Y.; Gatteschi, D.; Wernsdorfer, W. *Angew. Chem., Int. Ed.* **2003**, *42*, 1483–1486.
- (5) (a) Zheng, X. D.; Hua, Y. L.; Xiong, R. G.; Ge, J. Z.; Lu, T. B. *Cryst. Growth Des.* **2011**, *11*, 302–310. (b) Panja, A. *J. Coord. Chem.* **2011**, *64*, 987–995. (c) Venkatakrisnan, T. S.; Sahoo, S.; Bréfuel, N.; Duhayon, C.; Paulsen, C.; Barra, A. L.; Ramasesha, S.; Sutter, J. P. *J. Am. Chem. Soc.* **2010**, *132*, 6047–6056. (d) Zhang, W.; Sun, H. L.; Sato, O. *CrystEngComm* **2010**, *12*, 4045–4047. (e) Yoo, H. S.; Ko, H. H.; Ryu, D. W.; Lee, J. W.; Yoon, J. H.; Lee, W. R.; Kim, H. C.; Koh, E. K.; Hong, C. S. *Inorg. Chem.* **2009**, *48*, 5617–5619. (f) Choi, S. W.; Ryu, D. W.; Lee, J. W.; Yoo, H. S.; Kim, H. C.; Lee, H.; Cho, B. K.; Hong, C. S. *Inorg. Chem.* **2009**, *48*, 9066–9068. (g) Zhang, W.; Wang, Z. Q.; Sato, O.; Xiong, R. G. *Cryst. Growth Des.* **2009**, *9*, 2050–2053. (h) Zhang, D. P.; Wang, H. L.; Tian, L. J.; Ni, Z. H. *CrystEngComm* **2009**, *11*, 2447–2451. (i) Zheng, X. D.; Jiang, L.; Feng, X. L.; Lu, T. B. *Inorg. Chem.* **2008**, *47*, 10858–10865. (j) Jiang, L.; Feng, X. L.; Su, C. Y.; Chen, X. M.; Lu, T. B. *Inorg. Chem.* **2007**, *46*, 2637–2644. (k) Liang, S. W.; Li, M. X.; Shao, M.; Miao, Z. X. *Inorg. Chem. Commun.* **2006**, *9*, 1312–1314. (l) Jiang, L.; Lu, T. B.; Feng, X. L. *Inorg. Chem.* **2005**, *44*, 7056–7062. (m) He, X.; Lu, C. Z.; Yuan, D. Q.; Chen, S. M.; Chen, J. T. *Eur. J. Inorg. Chem.* **2005**, 2181–2188.
- (6) Pigué, C.; Bünzli, J.-C. G. In *Handbook on the Physics and Chemistry of Rare Earths*; Gschneidner, K. A., Jr., Bünzli, J.-C. G., Pecharsky, V. K., Eds.; Elsevier: Amsterdam, 2010; Vol. 40, Chapter 247, pp 534–539.
- (7) (a) Zhang, M. L.; Li, D. S.; Fu, F.; Yang, X. G.; Wu, Y. P.; Wang, E. B. *Inorg. Chem. Commun.* **2008**, *11*, 958–960. (b) Xiao, D. R.; Wang, E. B.; An, H. Y.; Li, Y. G.; Xu, L. *Cryst. Growth Des.* **2007**, *7*, 506–512. (c) Ye, J. W.; Zhang, P.; Ye, K. Q.; Ye, L.; Yang, G. D.; Wang, Y. *Chin. Sci. Bull.* **2006**, *51*, 1682–1686. (d) Luo, F.; Che, Y. X.; Zheng, J. M. *Inorg. Chem. Commun.* **2006**, *9*, 848–851. (e) Chen, X. M.; Liu, G. F. *Chem.—Eur. J.* **2002**, *8*, 4811–4817.
- (8) (a) Chen, X.; Zhou, H.; Chen, Y. Y.; Yuan, A. H. *CrystEngComm* **2011**, DOI: 10.1039/c1ce05699a. (b) Zhou, H.; Yuan, A. H.; Qian, S. Y.; Song, Y.; Diao, G. W. *Inorg. Chem.* **2010**, *49*, 5971–5976. (c) Yuan, A. H.; Qian, S. Y.; Liu, W. Y.; Zhou, H.; Song, Y. *Dalton Trans.* **2011**, *40*, 5392–5306. (d) Yuan, A. H.; Chu, C. X.; Zhou, H.; Yuan, P.; Liu, K. K.; Li, L.; Zhang, Q. F.; Chen, X.; Li, Y. Z. *Eur. J. Inorg. Chem.* **2010**, 866–871. (e) Yuan, A. H.; Southon, P. D.; Price, D. J.; Kepert, C. J.; Zhou, H.; Liu, W. Y. *Eur. J. Inorg. Chem.* **2010**, 3610–3614.
- (9) Kahn, O. *Molecular Magnetism*; VCH Publisher: New York, 1993.
- (10) Bok, L. D. C.; Leipoldt, J. G.; Basson, S. S. Z. *Anorg. Allg. Chem.* **1975**, *415*, 81–83.
- (11) Bruker. SMART, SAINT and XPREP: Area Detector Control and Data Integration and Reduction Software; Bruker Analytical X-ray Instruments Inc.: Madison, WI, 1995.
- (12) Sheldrick, G. M. SADABS: Empirical Absorption and Correction Software; University of Göttingen: Göttingen, Germany, 1999.
- (13) Sheldrick, G. M. SHELXS-97: Programs for Crystal Structure Solution; University of Göttingen: Göttingen, Germany, 1997.
- (14) Sheldrick, G. M. SHELXL-97: Programs for the Refinement of Crystal Structures; University of Göttingen: Göttingen, Germany, 1997.
- (15) (a) Alvarez, S.; Alemany, P.; Casanova, D.; Cirera, J.; Llunell, M.; Avnir, D. *Coord. Chem. Rev.* **2005**, *249*, 1693–1708. (b) Casanova, D.; Cirera, J.; Llunell, M.; Alemany, P.; Avnir, D.; Alvarez, S. *J. Am. Chem. Soc.* **2004**, *126*, 1755–1763. (c) Casanova, D.; Llunell, M.; Alemany, P.; Alvarez, S. *Chem.—Eur. J.* **2005**, *11*, 1479–1494. (d) Llunell, M.; Casanova, D.; Cirera, J.; Bofill, J. M.; Alemany, P.; Alvarez, S.; Pinsky, M.; Avnir, D. SHAPE, v. 1.1b; University of Barcelona: Barcelona, Spain, 2005.
- (16) (a) Ma, S. L.; Ma, Y.; Ren, S.; Yan, S. P.; Cheng, P.; Wang, Q. L.; Liao, D. Z. *Cryst. Growth Des.* **2008**, *8*, 3761–3765. (b) Lim, J. H.; You, Y. S.; Yoo, H. S.; Yoon, J. H.; Kim, J. H.; Koh, E. K.; Hong, C. S. *Inorg. Chem.* **2007**, *46*, 10578–10586. (c) You, Y. S.; Yoon, J. H.; Lim, J. H.; Kim, H. C.; Hong, C. S. *Inorg. Chem.* **2005**, *44*, 7063–7069. (d) You, Y. S.; Kim, D.; Do, Y.; Oh, S. J.; Hong, C. S. *Inorg. Chem.* **2004**, *43*, 6899–6901.
- (17) Gao, S.; Ma, B. Q.; Sun, H. L.; Li, J. R. *J. Solid State Chem.* **2003**, *171*, 201–207.
- (18) Zhao, H. H.; Lopez, N.; Prosvirin, A.; Chifotides, H. T.; Dunbar, K. R. *Dalton Trans.* **2007**, 878–888.
- (19) Spek, A. L. *J. Appl. Crystallogr.* **2003**, *36*, 7–13.
- (20) Janiak, C. *J. Chem. Soc., Dalton Trans.* **2000**, 3885–3896.
- (21) (a) Yan, C. F.; Chen, L.; Feng, R.; Jiang, F. L.; Hong, M. C. *CrystEngComm* **2009**, *11*, 2529–2535. (b) Dai, F. N.; He, H. Y.; Zhao, X. L.; Ke, Y. X.; Zhang, G. Q.; Sun, D. F. *CrystEngComm* **2010**, *12*, 337–340. (c) Wen, L. L.; Dang, D. B.; Duan, C. Y.; Li, Y. Z.; Tian, Z. F.; Meng, Q. J. *Inorg. Chem.* **2005**, *44*, 7161–7170.
- (22) (a) Liu, X. Q.; Liu, Y. Y.; Hao, Y. J.; Yang, X. J.; Wu, B. *Inorg. Chem. Commun.* **2010**, *13*, 511–513. (b) Yao, J. C.; Huang, W.; Li, B.; Gou, S. H.; Xu, Y. *Inorg. Chem. Commun.* **2002**, *5*, 711–714. (c) Zhang, Y. G.; Li, J. M.; Chen, J. H.; Su, Q. B.; Deng, W.; Nishiura, M.; Imamoto, T.; Wu, X. T.; Wang, Q. M. *Inorg. Chem.* **2000**, *39*, 2330–2336.
- (23) Przychodzeń, P.; Pełka, R.; Lewiński, K.; Supel, J.; Rams, M.; Tomala, K.; Sieklucka, B. *Inorg. Chem.* **2007**, *46*, 8924–8938.